

STRUCTURAL RESPONSE OF DN15-TUBES UNDER RADIOLYSIS GAS DETONATION LOADS FOR BWR SAFETY APPLICATIONS

M. Kuznetsov*

*Institute for Nuclear and Energy
Technology, Research Center Karlsruhe
PO. Box 3640, D-76021 Karlsruhe
Germany*
Phone: +49 7247-824716,
Fax: +49 7247-824777
e-mail: kuznetsov@iket.fzk.de

W. Breitung

*Institute for Nuclear and Energy
Technology, Research Center Karlsruhe
PO. Box 3640, D-76021 Karlsruhe
Germany*
Phone: +49-7247-822463,
Fax: +49 7247-824777
e-mail: breitung@iket.fzk.de

J. Grüne

*Pro-Science, Parkstrasse 9, 76275
Ettlingen, Germany*
Fax: +49 7243-537077
e-mail: grune@iket.fzk.de

R.K. Singh

*Reactor Safety Division,
Bhabha Atomic Research Center,
Trombay, Mumbai 400 085, India*
Fax: +91 22 25505151
e-mail: rksingh@magnum.barc.ernet.in

ABSTRACT

A U-shaped DN15 tube with 15 mm ID, 3 mm wall thickness was exposed to radiolysis gas ($2\text{H}_2+\text{O}_2$) detonation loads to investigate the structural stability of typical BWR tubes. Radiolysis gas at ambient temperatures was used at initial pressure up to 70 bar. The effect of transient detonation loads with peak pressures up to 1540 bar on the tube response was studied with strain gauges and simultaneous local pressure measurements.

The strain measurements demonstrated that the tube material remained in the elastic response regime for initial radiolysis gas pressures of up to 20 bar. For the case with 30 and 70 bar initial pressure, local plastic deformations were observed under peak detonation pressures of 540 and 1540 bar, respectively.

The measured strain values could be well explained with a simplified analysis of the elastic-plastic material behaviour under quasi-static loading conditions. Based on the measured strain data for the DN-15 tube, upper and lower bounds were estimated for the burst pressures of the failed pipes in the Brunsbüttel and the Hamaoka-1 NPP events.

The experiments provide new data for the validation of structural dynamic codes and models of the response of typical BWR tubes under radiolysis gas detonation loads.

Keywords: Radiolysis Gas, Detonation, Boiling Water Reactor, Elastic-Plastic Mechanical Response.

1. INTRODUCTION

Radiolysis gas is generated due to the enhanced water dissociation in a radiation field in the core of operating nuclear boiling water reactors (BWR). Steam leaving the core region generally has a concentration of 22 vol. ppm hydrogen and 11 vol. ppm oxygen. This means that at normal BWR conditions ($T = 560$ K and $p = 70$ bar) the mixture of radiolysis gas and steam is inert. A decrease of the radiolysis gas-steam temperature results in a

decrease of the steam content below the upper flammability limit (Schröder, 2003) (Fig. 1). The picture shows a saturated steam content at 70 bar of initial pressure. Below the flammability limit the mixture becomes combustible, and different flame propagation regimes are possible, depending on the actual steam concentration.

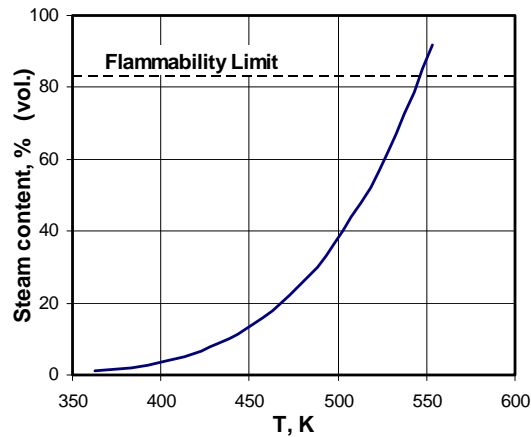


Fig. 1. Steam content for radiolysis gas vs. temperature ($p = 70$ bar)

The potential of the burned mixture for flame acceleration to sonic velocity with following detonation on-set can be estimated using the expansion ratio σ and the detonation cell size λ , correspondingly. Fig. 2 shows the dependence of the expansion ratio and the calculated detonation cell size of radiolysis gas/steam mixtures at the steam saturation against temperature at a fixed pressure of 70 bar.

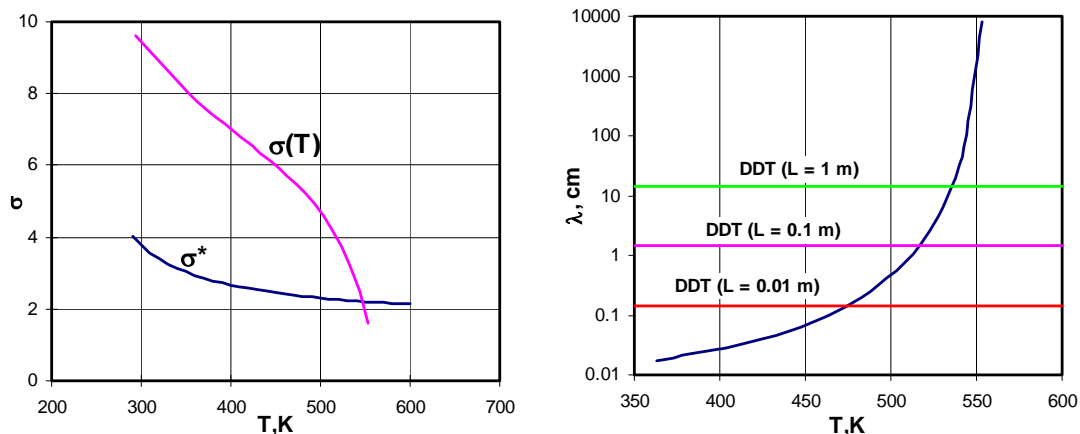


Fig. 2. Expansion ratio σ (left) and calculated detonation cell size λ (right) as a function of initial temperature of the radiolysis gas-steam mixture ($p = 70$ bar).

Effective flame acceleration was found to be possible if the expansion ratio σ of the mixture under consideration is larger than a certain critical expansion ratio σ^* , which is a function of the Zeldovich number β ($\beta = E_a(T_b - T_u)/T_b^2$) (Dorofeev, 2001). β represents a non-dimensional activation energy, which decreases with increasing initial temperature T_u and decreasing activation energy E_a . The critical expansion ratio σ^* was measured for hydrogen-air-steam mixtures under expected PWR accident conditions (Dorofeev, 2001). The result is shown in the left diagram of Fig. 2. For a first guess it may be assumed that the same σ^* -values apply for BWR-typical stoichiometric hydrogen- oxygen-steam mixtures, i.e. the same activation energy holds for both gas systems. The red line in Fig.2 (left) shows the calculated expansion ratio for $2H_2-O_2$ -steam mixtures as function of the initial temperature. At 300 K an almost pure stoichiometric hydrogen-oxygen mixture exists with a σ -value close to 10. Only mixtures with expansion ratios above σ^* can accelerate to supersonic flames. Mixtures with $\sigma(T) < \sigma^*$ do not provide a sufficiently strong expansion flow and only a subsonic combustion regime is possible. The extrapolation of the current data base leads thus to the conclusion that flame acceleration should become possible at temperatures below about 550 K.

Taking the 7λ criterion for detonation onset (Dorofeev, 1997; Dorofeev, 2000), a detonation becomes possible if the characteristic size $L > 7\lambda$, where λ is the detonation cell size (Gavrikov, 2000). The detonation cell size of radiolysis gas-steam mixture decreases rapidly with decreasing temperature (Fig. 2). For instance in a system with 10 cm characteristic dimension it may be expected that a mixture of radiolysis gas and saturated steam becomes detonable once the temperature dropped to about 520 K, which is only 40 degrees below the nominal operating temperature.

The detonation mode of combustion produces the maximum peak pressures. For example, theoretical estimations of the Chapman-Jouguet (CJ) detonation characteristics of radiolysis gas at the BWR operating pressure of 70 bar and a temperature of $T = 300\text{K}$ give pressure value of $P_{CJ} = 1504$ bar and detonation velocity of $D_{CJ} = 3070$ m/s. This high level of the pressure loads can result in disruption of mechanical structures. Recently two events with radiolysis gas explosions occurred in a Japanese and a German Boiling Water Reactors (Hamaoka-1 at November 7, 2001 and Brunsbüttel KKB, at December 14, 2001).

Fig. 3 shows views of pipes damaged by radiolysis gas detonations in both BWR accidents (Nakagami, 2002). The pipe deformations were analyzed in great detail after the accidents to examine the dynamic response of the pipe structure to the radiolysis gas detonation loads. In the case of Hamaoka-1, the pipe formed an S-shape, composed of two joined L-shaped parts (Fig. 3). The circumferential length ranged from approximately 103% to 107% compared to the original length. In the ruptured tube section the circumferential length was estimated as 123% of the reference value of the original carbon ferritic steel tube (165 x 11 mm size). The wall thickness was correspondingly reduced (Nakagami, 2002). Practically the same plastic deformation of 127% of the tube perimeter was observed as a result of the explosion in Brunsbüttel (austenitic stainless steel tube of 100 x 5.6 mm dimension) (Schulz, 2002).

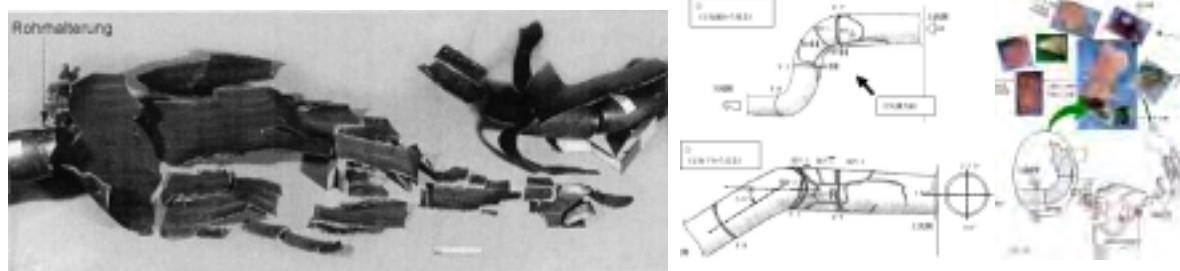


Fig. 3. Photographs of broken tubes as result of radiolysis gas detonations, left view: Brunsbüttel KKB, right view: Hamaoka-1 NPP.

The in-depth analysis of these two accidents showed that an extraordinary large pressure rise due to high speed combustion of radiolysis gas inside the pipes caused ductile material failure. The question is what the potential structural damage of such radiolysis gas detonations could be for steel pipes or other reactor components like valves and vessels.

Mechanical steel properties obtained under static pressure load are not valid for dynamic or impact loads, because the resistance to plastic deformation increases with the strain rate (Tang, 1965; Goldberg, 2004). That is, the tensile strain-stress curve can be shifted to higher stress values for the same strain by increasing the rate of strain during the test. For instance, the response of pipe structures to static and dynamic (detonation) loads studied by Luker (1959) showed that the critical dynamic peak pressure for steel diaphragm failure was one and half times higher than the corresponding value under static load. The effect of detonation waves in $\text{CH}_4 + 2.7\text{O}_2$ mixtures on tube failure was investigated by Randall (1960). They also observed that the measured failure stress was 1.5 times larger than calculated by the theory of thin cylindrical shells for a static pressure load.

An opposite behavior is typical for mechanical structures in elastic mode. Theoretical modeling of a mechanical structure as simple linear oscillator under dynamic load, showed that dynamic loads can result in up to two times larger displacements than the static load of the same peak pressure (Baker, 1983). The loading may be considered as quasi-static if the loading time is more than about six times the longest natural period. In this case the deformation depends only on the peak pressure (with amplification factor 2). This theory is in a good accordance with experimental data (Nettleton, 1979; Beltman, 1998). The amplification factor of a tube deformation under detonation load as a function of the Chapman-Jouguet pressure was changed from 2 to 3 in comparison with static load (Beltman, 1998).

2. OBJECTIVES

The objectives of this work were threefold:

(1) Investigation of the effect of radiolysis gas detonation pressures on the structural response of a U-shaped DN-15 stainless steel tube.

(2) Combined pressure and strain measurements during the steady-state detonation of radiolysis gas at different initial pressures (up to 70 bar).

(3) Investigation of deflagration-to-detonation transition (DDT) in a smooth tube for stoichiometric hydrogen-oxygen mixture at elevated initial pressures (1 - 70 bar) and ambient temperature ~300 K.

The primary goal of this experimental study was to investigate the detonation resistance of DN-15 tubes, which are installed frequently in German BWRs for instrumentation purposes. The tests addressed the most frequent geometrical configuration and the most probable ignition location, which is a DN-15 line with a relatively strong valve at the end and a weak ignition at this end. In such conditions DDT occurs within a short distance from the ignition point (e.g. few centimetres at 70 bar initial pressure) and a stable CJ-detonation propagates along the straight and curved pipes into the primary system. The effect of wave reflection was not addressed in this study because there are many different valve configurations used in German BWRs to terminate a DN-15 line.

3. EXPERIMENTAL DETAILS

Experiments on the structural integrity of a DN-15 tube (21.3 x 2.9 mm) with a typical U-shape geometry were performed using radiolysis gas. The tube of 6 m length was made from austenitic stainless steel WN 1.4541, similar to SS321 of the AISI/ASME steel standard (Fig. 3). The flanges and the wall near the flanges were reinforced to avoid a rupture of the flanges prior to a possible rupture of the cylindrical part of the tube and also to protect the cylindrical tube part close to the end against the strong reflected detonation wave. The DN-15 tube was located horizontally inside of safety vessel.

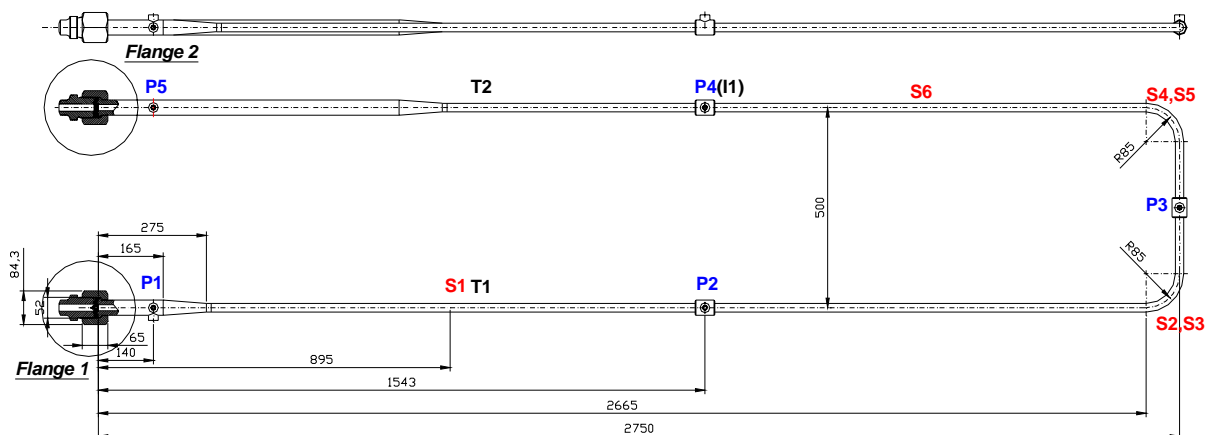


Fig. 3. The DN-15 test tube with denoting positions of pressure gauges, strain gauges and thermocouples.

Piezoelectric and piezoresistive pressure transducers P1-P5 were used to record the dynamic detonation pressures and to obtain run-up-distance of DDT process. The effect of the detonation loads on the tube response (straight and curved parts) was studied using strain gauges S1-S6 (2 or 3 elements scheme). The strain measurements were combined with simultaneous pressure measurements and post-test measurements of the tube dimensions. Two thermocouples T1 and T2 were mounted on the outer surface of the tube to measure the tube temperature before and after the detonation to prove the energy balance, as well as to clarify the temperature effect on the strain measurements. The locations of the gauges are shown in Fig. 3.

Stoichiometric hydrogen-oxygen mixtures at initial pressures from 0.5 to 70 bar and at temperatures of 290-300 K were used in the tests. The test mixture was prepared *in situ* by a precise flow rate control of hydrogen and oxygen. The ignition point in all the tests was located axially at the centre of flange 1 (Fig. 3). To avoid direct initiation of a detonation, the mixture was ignited by a glow plug.

3.1 Experimental Results and Discussion

3.1.1 Radiolysis gas detonation experiments

Detonation experiments with stoichiometric hydrogen-oxygen mixtures as a pure radiolysis gas have been performed at initial pressures from 0.5 to 70 bar. The main parameters obtained from the experimental data were run-up-distance, detonation pressure and detonation velocity. A comparison between the measured and theoretical Chapman-Jouguet detonation velocities indicates that the detonation has a steady-state character (Fig. 4). The measured peak pressures during the detonation are very close to the theoretical CJ-pressures. The maximum peak pressures at the last gauge, which was positioned close to the tube end, were about 1.2 - 1.4 times higher than the corresponding CJ-value due to wave reflection at the tube end.

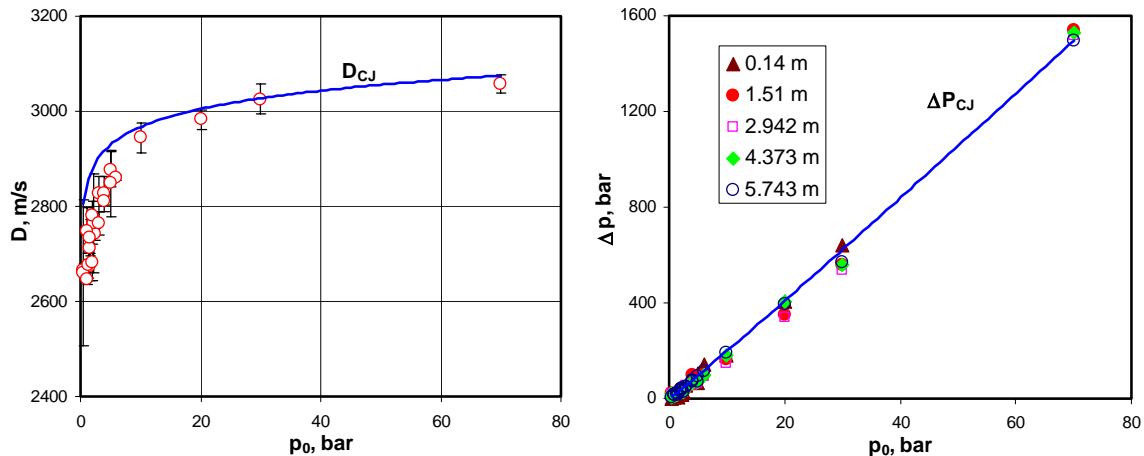


Fig. 4. Comparison of measured (points) and calculated (line) detonation characteristics: velocity (left); pressure (right).

The duration of the detonation pressure load is a very important parameter for the dynamic load regime. According to the pressure signals, the characteristic time of the positive pressure phase varied from about 5 to 10 ms.

An important parameter of detonation initiation in tubes is known as the distance to detonation onset or so-called run-up-distance. It corresponds to the smallest space required for turbulent flame acceleration and leading to shock formation followed by transition to detonation. The dependence of the run-up-distance r_D was found to be inversely proportional to the initial pressure p_0 to the power of 2/3:

$$r_D [\text{m}] = 0.42 \cdot p_0 [\text{bar}]^{-0.66}.$$

The run-up-distance for radiolysis gas at 70 bar initial pressure could be estimated as about 25 mm from the ignition point. According to this result at typical BWR pressure, a weak ignition of even very small amounts of radiolysis gas (a few cm characteristic lengths) could lead to a detonation.

3.1.2 Strain measurements

The structural response of the straight and the curved parts of the DN-15 tube was investigated using 6 strain gauges. The purpose of this investigation was to obtain experimental data for the dependence of strain versus pressure under highly dynamic detonation loads (10 - 1500 bar). Another important task was to investigate the magnitude of the tube deformation under detonation load to identify the safety margin available for such tubes. To study the mechanical tube response, data for the engineering strain $\varepsilon = \Delta L/L_0$ have been obtained for different detonation loads. Typical dependencies of measured strain ε versus time for an initial pressure of 70 bar and different locations are shown in Fig. 5.

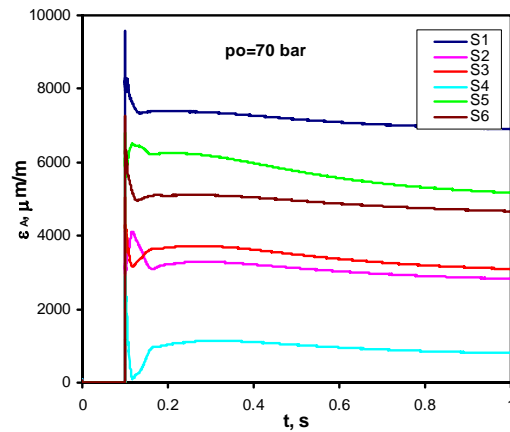


Fig. 5. Typical strain records vs. time ($p_0 = 70$ bar).

Two characteristic phases of the mechanical response to the detonation load can be distinguished on basis of the strain signal (Fig. 5): 1) a fast response period; 2) a relaxation period. The fast response period corresponds to the pressure load of the detonation wave (~10 ms). The time of maximum strain value coincides almost exactly with the time of arrival of the peak detonation pressure. The characteristic response time of the tube structure to the dynamic pressure load was 5-10 μ s. It corresponds to the strain rate 100-1000 s^{-1} .

The relaxation period has a typical duration of 200 to 300 ms after arrival of the detonation wave. During this later period the maximum strain was found to be in accordance with the thermal expansion coefficient of stainless steel (16 μ m/(m·K)). After the relaxation phase, a cooling of the heated tube due to thermal exchange with ambient air takes place.

The measured maximum circumferential strain values are presented in Fig. 6 as a function of maximum detonation peak pressure in range 10-1500 bar. At initial pressures up to 30 bar the maximum strain was measured in the curved parts of the tube (gauges S2 - S5). However, for the initial pressure of 70 bar the maximum strain values correspond to gauge positions on the straight parts of the tube (gauges S1 and S6). It appears that during 30 bar initial pressure experiment the bend regions of the tube reached the yield limit (0.1 % strain) locally and hence the resulting strain hardening caused less elastic strain compared to the straight part of the tube where the tube was driven to the plastic regime due to its original condition in the 70 bar initial pressure experiment.

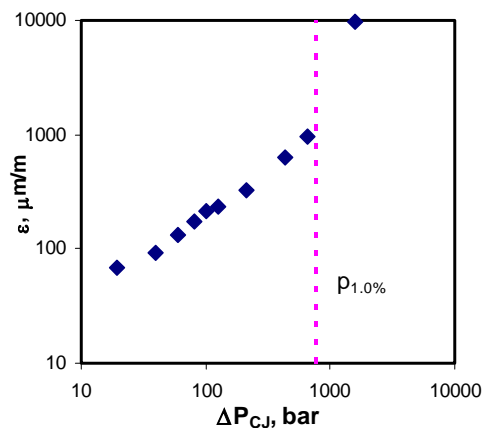


Fig. 6: Dependence of maximum strain vs. detonation peak pressure:
 $p_{1.0\%} = 770$ bar for static pressure load corresponding to 1% strain.

For the initial pressures from 0.5 to 30 bar, the maximum strain values are related to the maximum detonation pressure according to

$$\epsilon_{max}[\mu\text{m/m}] = (2.8-3.4) \cdot \Delta P_{CJ}[\text{bar}]^{(0.85-0.88)}.$$

This relation is almost linear and gives evidence that the material was mainly in elastic regime. In the 70 bar test the maximum strain was found to be several times higher than predicted by the above relation. This is very likely due to the beginning of plastic deformation under the high detonation load from 70 bar initial pressure. In case of the lower initial pressures (<30 bar) the tube remained in the elastic response regime.

The direct measurements of the permanently residual deformations show that after detonations with initial pressures less than 30 bar, the tube diameter was essentially unchanged (less than $\pm 0.05\%$ change). This means that for these initial pressures, only recoverable elastic deformations of the tube component occurred. The measurements of the tube dimensions after the detonation with an initial pressure of 70 bar showed, that the remaining deformations varied from 0.2% to 0.65%. The highest remaining deformations (0.5-0.65%) were observed in the straight parts of the tube towards both the tube ends. Smaller permanent deformations (0.2%) have been observed in the curved parts of the tube. This is in a good agreement with the maximum dynamic strain values measured by the strain gauges.

A maximum strain value of about 1% was recorded in position S1 (straight part). A calculation of the maximum static pressure corresponding to 1% strain for the test tube gives a value about 770 bar. The dynamic peak detonation pressure (about 1500 bar) at which 1% strain was reached is at least twice as high as the calculated static pressure value 770 bar (Fig. 6). This is in accordance with data (Goldberg, 2004) for high strain load. At the detonation peak pressure about 770 bar, actually only 0.1% strain was achieved experimentally. Thus, we should consider the effect of transient load on tube structure using strain data analysis for dynamic detonation load.

3.1.3 Strain data analysis for dynamic detonation load and collapse pressure prediction.

The transient loading regime of a structure is often characterized by comparing the duration of the load with the longest natural period of the loaded structure. A simplified analysis has been made to correlate the measured strain data with the predicted strain values for dynamic detonation load.

With the given tube data the circular frequency for the breathing mode is by Blevins (1995)

$$\omega = \sqrt{\frac{E}{\rho(1-\nu^2)}} = 5.8 \cdot 10^5 \text{ sec}^{-1},$$

where $E = 2.05 \times 10^5$ MPa, Young's modulus of elasticity; $\rho = 7950 \text{ kg/m}^3$, density; $\nu = 0.3$, Poisson's ratio; $r = 9.2$ mm, mean tube radius. The quasi-static loading regime is given for $\omega\tau \sim 40$ ($\tau =$ pulse duration). Pulse duration of $\tau > 40/\omega$ can produce a quasi-static response with amplification (Baker, 1983). This gives $\tau \sim 6.9 \cdot 10^{-5}$ sec. A detonation pressure pulse with a characteristic time of 10 ms as obtained in this work would be quasi-static because the pulse duration is above the period $\tau = 6.9 \cdot 10^{-5}$ sec.

Theoretical modeling of a mechanical structure, as simple linear oscillator under dynamic load, showed that dynamic loads can result in up to two times larger displacements than the static load of the same peak pressure or dynamic load factor up to 2 for quasi-static case (Baker, 1983). This theoretical prediction is in accordance with our experimental data. For example, the maximum circumferential strain recorded in the test at initial pressure 10 bar was $360 \mu\epsilon$ for a pulse duration of 10 msec. Circumferential stress $\sigma_\theta = 2P_{CJ}/(k^2-1) = 41$ MPa for CJ-pressure $P_{CJ} = 18$ MPa and $k = b/a = 1.374$. For the DN-15 tube $b = 10.65$ mm, outer radius; $a = 7.75$ mm, inner radius. The nominal circumferential strain for elastic deformations $\epsilon_0 = \sigma_\theta/E = 200 \mu\epsilon$. Thus, for the quasi-static regime the amplification factor is $360/200 = 1.8$. This is consistent with the amplification factor for a triangular pulse to which the present pulse can be approximated quite well.

Initial pressure 20 bar: The maximum circumferential strain recorded in the test is $774 \mu\epsilon$ with a pulse duration of ~ 9 msec. Circumferential stress $\sigma_\theta = 79.4$ MPa for CJ-pressure $P_{CJ} = 35$ MPa. The nominal circumferential strain $\epsilon_0 = 387 \mu\epsilon$. So for the quasi-static regime the amplification factor is $774/387 = 2.0$. This is again consistent with the amplification factor ~ 2 for an approximately triangular pulse in the quasi-static regime.

Initial pressure 30 bar: Circumferential stress $\sigma_\theta = 122$ MPa for CJ-pressure $P_{CJ} = 54$ MPa. The nominal circumferential strain $\epsilon_0 = 595 \mu\epsilon$. The maximum circumferential strain recorded in the experiment is $1260 \mu\epsilon$. This illustrates that the tube deformed in the inelastic regime due to the dynamic amplification with strain more than $1000 \mu\epsilon$ (0.1%), which is the elastic limit. It also explains the relatively low strain values in the bent segment of the tube compared to the straight part observed in the 70 bar test. The strain hardening of the curved tube section in the 30 bar experiment leads to the observed reversal of the strain profile for the 70 bar test, with the largest strain values in the straight parts of the tube (gauges S1, S6).

To obtain the amplification factors in the elastic and inelastic regimes the following evaluation is made using the stress-strain diagram shown below. The local tangent modulus from stress-strain curve for SS-321 material is (Materna-Morris 2002):

$$E_T = 3.6 \cdot 10^4 \text{ MPa,}$$

Hardening parameter

$$H' = \frac{E_T}{1 - E_T/E} = 4.4 \cdot 10^4 \text{ MPa.}$$

With a strain amplification of ~ 2 in the elastic region the observed plastic strain $\Delta \varepsilon^P = 630 \cdot 2 - 1000 = 260 \mu\varepsilon$. Out of the total strain of $1260 \mu\varepsilon$ the elastic strain has an amplification of 2: $1000/500 = 2$. For the remaining $95 \mu\varepsilon$ (out of total nominal circumferential strain $595 \mu\varepsilon$) the amplification factor would be $260/95 = 2.74$. This higher amplification for plastic strain is consistent with dynamic load factors found for simplified ideal elastic-plastic response.

The total stress developed during the 30 bar experiment is

$$\sigma = \sigma_y + \Delta \sigma = \sigma_y + H' \Delta \varepsilon^P = 216 \text{ MPa}$$

Thus, the yield stress for the subsequent experiment would be 216 MPa.

Initial pressure 70 bar: Circumferential stress $\sigma_\theta = 351 \text{ MPa}$ for CJ-pressure $P_{CJ} = 154 \text{ MPa}$. Current yield stress from 30 bar test $\sigma'_y = 216 \text{ MPa}$. $\Delta \sigma = \sigma_\theta - \sigma'_y = 135 \text{ MPa}$. Nominal plastic strain on subsequent loading $\Delta \varepsilon^P = \Delta \sigma / H' = 3068 \mu\varepsilon$. The maximum circumferential strain recorded in the experiment is $1260 \mu\varepsilon$. Chapman-Jouguet pressure $P_{CJ} = 1540 \text{ bar} = 154 \text{ MPa}$. Assuming again dynamic amplification of 2 for elastic strain the observed plastic strain during the experiment is

$$\Delta \varepsilon^P = 9585 - \sigma_y / E = 8529 \mu\varepsilon$$

The dynamic amplification for the plastic strain = $8529/3068 = 2.78$. This higher amplification factor for plastic strain is consistent with simplified ideal plastic dynamic load factors.

The above calculations demonstrate that the 10 bar and 20 bar experiments resulted only in elastic response of the tube with dynamic strain amplification of ~ 2 . For the 30 bar experiment the response was in the elastic-plastic regime and a higher strain amplification of about 2.74 was observed for the plastic strain component. In case of the 70 bar test, the material was already strain hardened near the tube bends and on the subsequent loading a higher strain was observed in straight parts of the tube, compared to the curved parts. In this case a plastic strain amplification factor of ~ 2.78 was observed. The reported shock spectra for the elastic-plastic regime are based on ideal elastic-plastic material behavior but a higher strain amplification (compared to 2 for the elastic regime) is justified if strain hardening characteristics are taken into account.

In the above calculations the strain rate effects have been neglected. The observed maximum strain rate is computed for these experiments: $\dot{\varepsilon} = \varepsilon / \tau \sim 1000 \text{ sec}^{-1}$, where $\varepsilon = 9585 \mu\varepsilon$, the maximum strain; $\tau = 1 \times 10^{-5} \text{ s}$, characteristic time for 70 bar experiment. For $\dot{\varepsilon} \sim 1000 \text{ sec}^{-1}$ the influence on mechanical properties of SS321 steel are shown to be almost insignificant (Materna-Morris 2002). Thus, the above presented simplified evaluation of the experiments appears justified.

3.1.3 Burst pressure evaluation.

For the DN-15 tube the lower bound burst pressure is evaluated based on flow stress which is the mean of yield stress and ultimate stress:

$$p^L = \sigma_f \ln \frac{b}{a} = 133 \text{ MPa.}$$

The evaluation of an upper bound burst pressure is based on the ultimate stress σ_u :

$$p^u = \sigma_u \ln \frac{b}{a} = 200 \text{ MPa.}$$

Using the above estimations for the lower and upper burst pressures, we obtain the following results for the present DN-15 tube and the tubes, which failed in the Brunsbüttel and Hamaoka NPPs (Table 1).

Table 1: Lower and upper burst pressure estimation.

Scenario	DN-15 pipe	Brunsbüttel NPP	Hamaoka NPP
Inner radius a (mm)	7.75	44.4	71.5
Outer radius b (mm)	10.65	50	82.5
$k = b/a$	1.374	1.126	1.154
Material	Stainless steel SS321	Stainless steel SS321	Ferritic carbon steel
Yield stress σ_y (MPa)	205	205	205
Ultimate stress σ_u (MPa)	630	630	450
Flow stress σ_f (MPa)	417.5	417.5	327.5
Lower bound burst pressure p^L (MPa)	132.7	49.6	46.9
Upper bound burst pressure p^u (MPa)	200.3	74.8	64.4

The Table 1 indicates that the reported failures of the Brunsbüttel and Hamaoka pipes can be explained with the upper and lower bound estimations for the burst pressure. It is clear that the maximum burst pressure for these tubes are much smaller than the peak detonation pressure (P_{CJ}) from detonation at 70 bar initial pressure, which was found to be ~ 156 MPa in the experiment. The investigated DN-15 tube could survive at this pressure because P_{CJ} of 156 MPa is between the two limiting estimations of 132.7 MPa and 200.3 MPa. The tubes of the two NPP's have relatively low burst pressures due to the large radius-to-thickness ratio. These tubes have been designed with large safety factors for the operating pressure of 7 MPa and not for radiolysis gas detonation loads.

4. CONCLUSIONS

The conditions for DDT in stoichiometric hydrogen-oxygen mixtures have been studied experimentally in a smooth DN-15 tube for a wide range of initial pressures (0.5 – 70 bar) at ambient temperature (about 300 K).

The U-shaped DN-15 test tube withstood dynamic loads from stable unreflected CJ detonations of radiolysis gas up to 70 bar initial pressure without mechanical failure (initial temperature about 300 K). In the 70 bar experiment the CJ peak detonation pressure was close to 1500 bar.

The tube remained in the elastic response regime up to 20 bar initial radiolysis gas pressure. For 30 and 70 bar initial pressure local plastic deformations occurred. In the 70 bar experiment local transient deformations up to about 1% strain were measured.

The measured strain values can be well explained with a simplified analysis of the elastic and plastic material behaviour.

The peak detonation pressure leading to 1% strain was about 2 times higher (1500 bar) than the estimated static pressure for the same yield (700 to 800 bar).

The tube response is in the quasi-static loading regime. Amplification of the dynamic tube response with factors of about 2 for the elastic strain and factors of about 2.75 for the plastic strain was found under detonation loads.

Based on the new measured strain data, upper and lower bounds were estimated for the burst pressures of the failed Brunsbüttel and Hamaoka pipes. It was shown that the expected burst pressures for these tubes are much smaller than the peak pressure (P_{CJ}) from radiolysis gas detonation at 70 bar initial pressure, which explains the failure mechanism in the plants.

REFERENCES

- Baker, W.E., Cox, P.A., Westine, P.S., Kuletsz, J.J., Strehlow, R.A., (1983) "Explosion Hazards and Evaluation", Elsevier, Amsterdam-Oxford-New York
- Beltman, W.M., Shepherd, J.E., Burcsu, E.N., and Zuhail, L., (1998) GALCIT Report FM 98-3
- Blevins R D, (1995) "Formulas for natural frequencies and mode shapes", Krieger publishing Co., Florida.
- S.B. Dorofeev, M.S. Kuznetsov, V.I. Alekseev, A.A. Efimenko, W. Breitung, (2001) J. Loss Prev. Proces. Ind.,

Vol.14, pp.583-589.

Dorofeev, S., Sidorov, V., Dvoinishnikov, A., Denkevits, A., Efimenko, A., and Lelyakin, A., (1997) Report RRC KI 80-05/16.

S.B. Dorofeev, V.I. Sidorov, M.S. Kuznetsov, I.D. Matsukov, V.I. Alekseev, (2000) Shock Waves, Vol.10, pp.137-149.

A.I. Gavrikov, A.A. Efimenko, S.B. Dorofeev, (2000) Combustion and Flame, Vol.120, pp.19-33.

Goldberg, R.K., Roberts, G.D., (2004) NASA Glenn's Research & Technology report

Materna-Morris, E., Graf, P., Zimmermann, H., Malmberg, T., (2002) Forschungszentrum Karlsruhe, Wissenschaftliche Berichte, FZKA 6525.

Nakagami, M., (2002) Chubu Electric Power Co., Inc., Japan, Report

M.A. Nettleton, (1979) J. Occ. Acc., Vol.2, p.99 (1979)

P.N. Randall, and I. Ginsburgh, (1960) ASME Trans. Paper No. 60-WA-12.

Schröder, V., Beckman-Kluge, M., (2003) Berlin, BAM- Projects 0202-II-0053.

H. Schulz, A. Voswinkel, H. Reck, (2002) Eurosafe, Forum for nuclear safety, Berlin 2002, GRS/IRSN

S. Tang, (1965) ASCE, J. Eng. Mech. Div., Vol. 91, p.97.